Available online at www.sciencedirect.com

ScienceDirect

Energy Procedia 81 (2015) 440 – 449

Energy Procedia

69th Conference of the Italian Thermal Engineering Association, ATI 2014

Small scale ORC plant modeling with the AMESim simulation tool: analysis of working fluid and thermodynamic cycle parameters influence.

M. Antonelli*, A. Baccioli, M. Francesconi, P. Psaroudakis, L. Martorano

Università di Pisa, D.E.S.Te.C., Largo Lucio Lazzarino, Pisa 56122, Italy

Abstract

ORC plant transient modeling is an actual issue for the correct assessment of the size of the various components of the system especially when unpredictable fluctuations of the inlet thermal flux are to be considered. This work shows the modeling procedure of a small scale (10-50 kW) Waste Heat Recovery ORC plant which uses an innovative expansion device derived from a Wankel engine. The numerical model here presented was developed with the simulation tools AMESim and simulates the transient behavior of such a small scale system in all its main components: preheater, evaporator, expansion device and condenser. The aims of this work were to evaluate the suitability of the Wankel-derived mechanism to ORC systems and to establish its optimal working conditions for the employment in a low-grade heat recovery system.

The application of several working fluids as well as of various operating conditions are presented in this paper. The analysis of the transient response of the plant is also presented with a particular attention to start up operations.

Peer-review under responsibility of the Scientific Committee of ATI 2014

Keywords: ORC cycles, Waste Heat Recovery, Micro-generation, Volumetric Expanders, Numerical Model, AMESim;

1. Introduction

The interest in low grade heat conversion to electricity has been strongly increasing in the last years to exploit renewable energies and recover the waste heat from industrial processes. The most studied technologies for the low

* Corresponding author. Tel.: +39-050-2217133; fax: +39-050-2217160.
E-mail address: marco.antonelli@ing.unipi.it

Peer-review under responsibility of the Scientific Committee of ATI 2014
doi:10.1016/j.egypro.2015.12.118

grade heat conversion to electricity are ORCs cycles, which are suitable for this field because of their simplicity and limited plant costs, the high efficiency at low temperature and the wide range of thermal power and temperature interval they can be combined.

For each application it is important to choose the most appropriate fluid. Quoilin et al in [1] determined the operating maps of various working fluids, as a function of the evaporating and condensing temperature, for three different expansion device. Antonelli et al [2] showed that different fluids applied to the same expander are able to cover a wide range of thermal power, only by changing the admission and recompression grade.

According to many authors, the strictest criterion for fluid selection is the ODP value of the fluid. Rayegan et al in [3] first of all discarded all the chlorine included fluid. Then they proceeded to choose the most suitable fluid for the plant.

Many applications, such as solar thermal and waste heat recovery are characterized by a variable temperature and mass flow rate over time, which need to be controlled by the thermodynamic cycle. For these systems the optimal working condition can differ by the stationary conditions and an optimal control strategy must be defined. For this sake, some authors [4] employed a dynamic model of a Waste Heat recovery ORC equipped with a Scroll device and compared different control strategies respect to the recovery efficiency.

For low scale cycles, the employment of volumetric devices is often hypothesized, due to their low rotational speed, low cost and high reliability and isentropic efficiency. Moreover they can bear a wide range of thermal power, under different pressure ratios and rotational speeds [5].

In this work the numerical model of a rotary volumetric device of the Wankel type was used to compare three different fluids, R-245fa, R600a and R-152a, in the temperature range 100-200°C and with thermal power up to 200 kW. Transient simulations were then performed to define the best control strategy respect to the power output, when temperature and mass flow rate are variable over time.

Nomenclature

T	Temperature, K
t	Time, s
$\dot{Q}$	Thermal power, kW
h	Specific enthalpy, KJ/kgK
ρ	Density, kg/ m^3
$\dot{m}$	Mass flow rate, kg/s
ε	Heat exchanger efficiency
W	Mechanical power, kW
η	Efficiency
$\dot{V}$	Volumetric flow rate, m^3/s
C_p	Constant pressure specific heat capacity, kJ/KgK
τ	Simulation time
R	Gas constant, kJ/kgK
$\dot{I}$	Exergy loss, kW
$\dot{S}$	Entropy flow rate, kW/K
s	specific entropy, kJ/kgK

Subscripts

e	Exchanged
a	Admission
p	Pump
fg	Flue gas
exp	Expander
g	Generated
0	Reference

2. Fluid selection

Fluid selection was performed in stationary conditions through the numerical model of the Wankel expander created with the simulation tool Amesim v.12, and already presented and validated by experimental results by Antonelli et al [2, 6 - 9]. The admission grade was kept constant to 0.2, to limit the thermal power within nearly 200 kW which was the target of this work. In each simulation, the rotational speed was varied in the range between 1500 and 3000 rpm, which is the typical working range of this type of expander.

Three different fluids were tested: R600a, R245fa and R152a.

The temperature of the superheat was in the range of 100-200°C for each fluid. As for the saturation temperature, it is useful to remind that the higher is the saturation temperature the higher is the cycle efficiency and the power output; near the critical point, however, small changes in temperature lead to large changes in pressure making the system unstable. Moreover, in a volumetric device for a fixed introduction grade and therefore for a fixed built in ratio [1] there is no convenience to adopt high saturation pressure, which can lead to under-expansion and therefore to power losses.

In the case of a turbine, to avoid droplets formation, some authors [3] reported that the saturation temperature may be chosen considering the slope of the saturation curve on the temperature entropy diagram, while others [10] suggested limiting the saturation temperature 10 or 15°C below the critical temperature. This last criterion was preferred in this work, since rotary devices are less sensitive to droplets formation. Moreover, since the thermal power range was limited to 200 kW, the saturation temperatures which led to a thermal input exceeding this limit were not taken into account. The saturation temperatures ranges for each fluid are reported in tab. 1. The condensing temperature was in every case equal to 35°C, assuming the use of a water-cooled condenser. The delivered power was evaluated for every fluid as a function of the superheating temperature and of the thermal power at the maximum saturation temperature (fig. 1-3).

Table 1. Saturation temperature ranges.

	R600a	R245fa	R152a
Tsat max [°C]	120	130	100
Tsat min [°C]	100	100	85

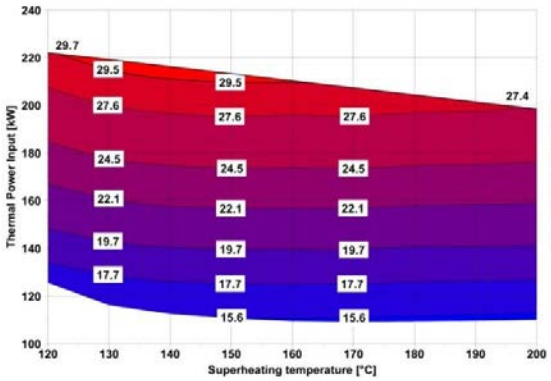

Fig. 1. R600a output power map.

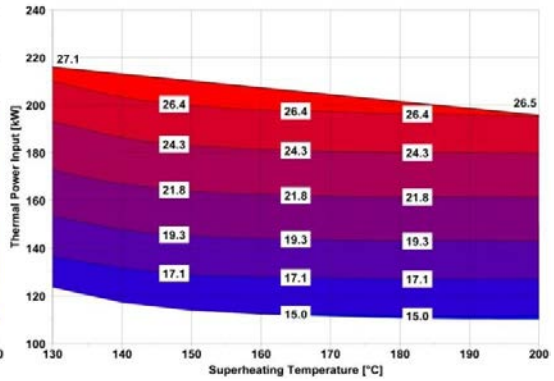

Fig. 2. R245fa output power map.

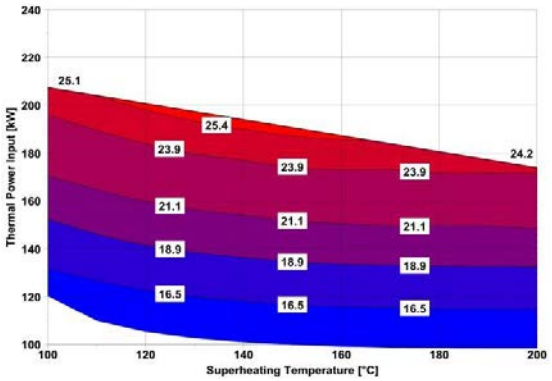

Fig. 3. R152a output power map.

For each fluid, thermal power and delivered power were found to be decreasing with the superheating temperature, due to the decrease of the density and therefore of the intake mass flow rate of the device.

Assuming that the exchange efficiency was the same for the three fluids, delivered power was the quantity that should be maximized in a waste heat recovery system for the same thermal power, as stated by [11].

R600a provided the highest delivered power among the three fluids and it was consequently selected for the transient analysis of the waste heat recovery system.

3. Dynamic numerical model

The dynamic model of the waste heat recovery ORC cycle (fig. 4) was developed using the pneumatic library and the two phase library of the simulation tool AMESim v.12. The hot stream was composed by flue gas with a variable over time mass flow rate and temperature, according to two load cycles (fig 5). The differences between these load cycles were in the amplitude of temperature variations, while mass flow rate was the same.

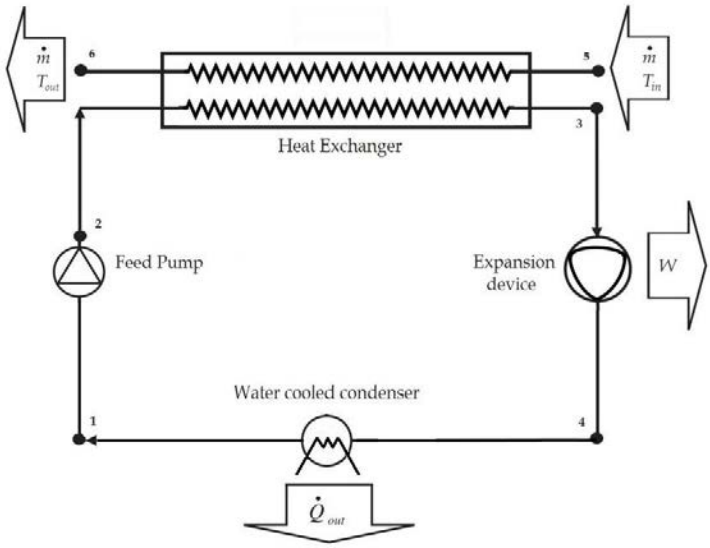

Fig. 4. Plant layout.

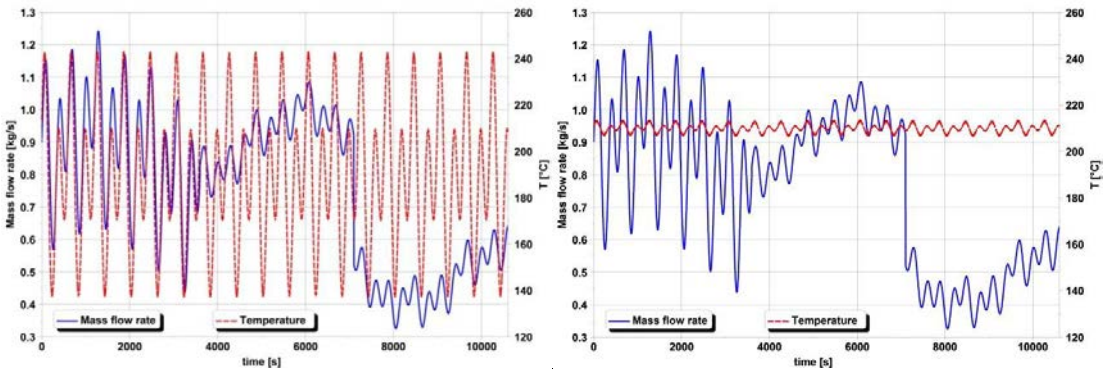

Fig. 5. Load cycle 1 (left) and 2 (right).

3.1.Heat exchangers

The economizer and the evaporator were hypothesized to be of shell and tube type. Components of pneumatic, thermal and two phase flow libraries were adopted for the simulation of the flue gas line, of the conduction through the walls of the heat exchanger and of the organic fluid. Their total volume was 100 liters.

The submodel of a phase separation chamber was used for the condenser. Temperature inside the chamber was kept constant to 35°C.

The recuperator was not employed since this device besides increasing the plant costs, increases the temperature at which the organic fluid enters into the heat exchanger causing a loss of exchanged thermal power, despite a little increase of the cycle efficiency.

3.2.Expansion device

For the sake of modelling the expansion device, the "two phase turbine" model was chosen. This model was calibrated by means of the volumetric flow rate and isentropic efficiency as a function of the pressure ratio, at different rotational speeds. These data were gathered from the results of the already cited expansion device numerical model [2, 6 - 9]. The fitted surface of the volumetric flow rate is reported in fig. 6.

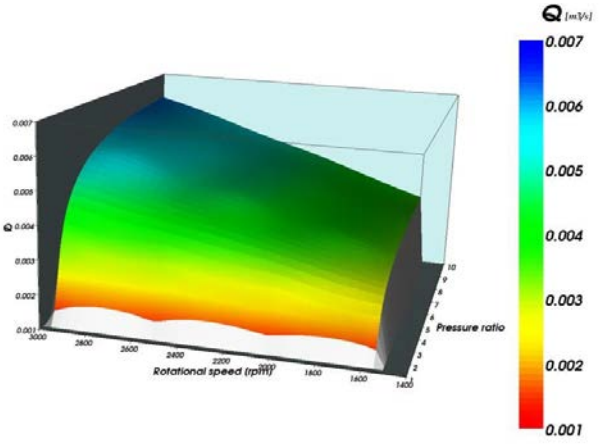

Fig. 6. Expander volumetric flow rate as a function of the pressure ratio and of rotational speed.

3.3.Pump

The pump was modelled as a volumetric fixed displacement pump with a constant efficiency ($\eta_p = 0.8$) and the work consumption was calculated as

$$W_{pump} = \frac{\dot{m} \times \Delta P}{\rho \times \eta_p} \quad (1)$$

The pump rotational speed was regulated by the liquid volume percentage into the evaporator.

3.4.Thermodynamics equation

The total heat transferred was computed using the temperature difference of the flue gas between the inlet and the outlet of the heat exchanger. Referring to fig. 3 the heat exchanged is

$$\dot{Q}_e = \dot{m}_{fg} \times \bar{C}_p \times (T_5 - T_6) \quad (2)$$

The exergy loss in the heat exchange was:

$$\dot{I}_e = T_0 \times \Delta\dot{S}_g = T_0 \times \left[\dot{m}_{fg} \times \left(\bar{C}_p \times \ln\left(\frac{T_5}{T_6}\right)\right) - R_{fg}\ln\left(\frac{P_5}{P_6}\right) - \dot{m}(s_3 - s_2)\right] \quad (3)$$

And the average exergy loss over the heat exchanger was

$$\bar{\dot{I}}_e = \frac{1}{\tau} \times T_0 \times \int_0^\tau \Delta\dot{S}_g \, dt \quad (4)$$

Where T_0 is the temperature of the reference environment set to 293K. The average exergy efficiency was calculated

$$\bar{\eta}_{II} = \frac{\int_0^\tau (W_{exp} - W_p) dt}{\int_0^\tau \dot{m}_{fg} \times \left[\bar{C}_p \times (T_5 - T_0) - T_0 \times \left(\left(\bar{C}_p \times \ln\left(\frac{T_5}{T_0}\right)\right) - R_{fg}\ln\left(\frac{P_5}{P_0}\right)\right)\right] dt} \quad (5)$$

4. Control implementation and plant management

As already mentioned, three different control strategies were compared respect to the overall recovery efficiency. The first strategy was to keep constant the rotational speed of the expander and leave to be free of varying the saturation pressure. The second strategy was to set a fixed saturation temperature and vary the rotational speed of the expander. In this strategy a constant set point for the evaporating temperature was defined. The difference between the set point and the actual saturation temperature, i.e. the error, was then used to drive the expander speed through an appropriate transfer function with a proper value of the gain for stability reasons. In this case an inverter was hypothesized to accommodate the device rotational speed, which was limited to the range 500-3000rpm. The third strategy consisted in a variable set point for the evaporating temperature in the range 100-120°C for the previously explained reasons. The optimal set point respect to the work output was calculated through a function of the volumetric flow rate and of the admission pressure, which was obtained through the results of the stationary model of the Wankel device. Different functions were estimated using both linear regression and quadratic regression and eventually the optimum function was found.

$$T_{set\ point} = -5848 \times \left(\dot{V} \times P_a\right)^2 + 1713.5 \times \left(\dot{V} \times P_a\right) + 32.4 \quad (6)$$

5. Discussion and Results

5.1 Superheated cycles.

The performances of the plant were evaluated both using superheated and saturated cycles in the range of saturation temperatures between 100-120°C.

Superheated cycles provided lower average net mechanical power, exchanged thermal power and overall efficiency than saturated cycles (fig. 7 - 8), both in the case of steady and transient conditions. On the other hand, as expected, saturated cycles involved a larger exergy loss (fig. 9) than superheated because of the worse match between the exchange curves. The effect of the use of superheated cycles was however a lower overall efficiency of the waste heat system.

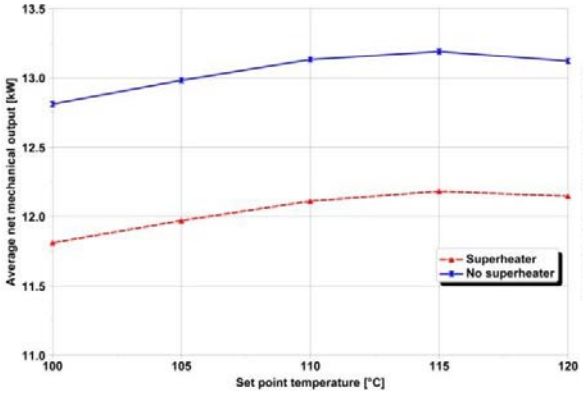

Fig. 7. Net average power output.

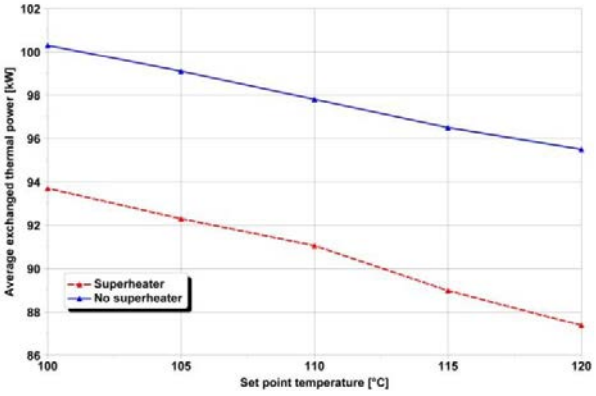

Fig. 8. Exchanged average thermal power.

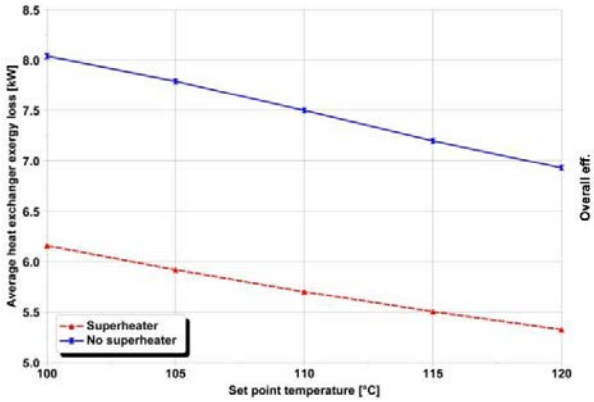

Fig. 9. Average heat exchanger exergy loss.

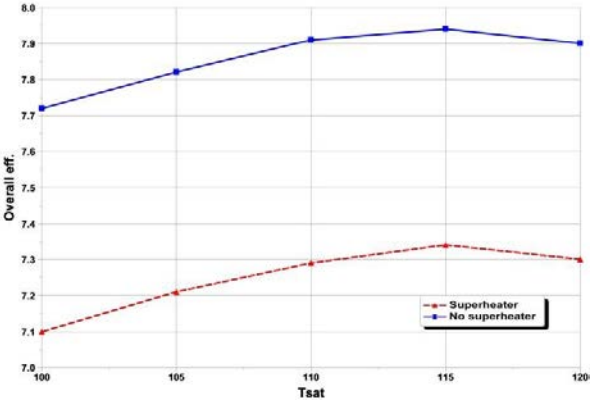

Fig. 10. Overall efficiency.

5.2.Control strategy comparison

The results of the above described control strategies were compared on the basis of averaged quantities for both load cycles, as reported in tab. 2 and 3, using a saturated cycle.

Table 2. Comparison of the strategies.

Load Cycle 1	Strategy I @ 2500 rpm	Strategy II @ Tsat= 115°C	Strategy III
Average net power output [kW]	12.13	13.19	13.21
Exchanged heat [kW]	109.28	95.5	97.1
Average second law efficiency [%]	41.65	49.37	49.79
Average overall efficiency [%]	7.31	7.94	7.96

Table 3. Comparison of the strategies.

Load Cycle 2	Strategy I @ 2500 rpm	Strategy II @ Tsat= 115°C	Strategy III
Average net power output [kW]	14.71	15.66	15.66
Exchanged heat [kW]	119.59	114.30	114.32
Average second law efficiency [%]	43.18	47.82	47.83
Average overall efficiency [%]	8.38	8.92	8.92

The first control strategy provided the lowest overall and second law efficiencies. Moreover if the rotational speeds rose above 2500 rpm the work output strongly decreased while on the other hand at low rotational speeds the saturation temperature approached and eventually exceeded its critical value. This strategy is therefore suitable only in the case of limited load variations. The second strategy provided good results only when the set point was properly tuned. In the other cases, which were not reported in the tables, the power output and the overall efficiency decreased. This type of regulation is suitable only in the cases in which the optimal value of the set point could be defined a priori.

The third type of regulation provided the maximum power output and overall efficiency with both the load cycles, similar to other published researches [4]. This type of regulation is suitable for those systems characterized by marked and unpredictable fluid mass flow rate and temperature variations. If compared to fixed set point strategies, the device rotational speed showed the minor fluctuations (fig. 11). At the saturation temperature of 100°C and 110°C the expander reached, on the contrary, the maximum allowed speed; in these cases the expander was not able to keep the evaporating temperature to the value defined by the set point. At the same time, using strategy 3, the plant proved to be able to follow the temperature set point for both diagrams (fig.12).

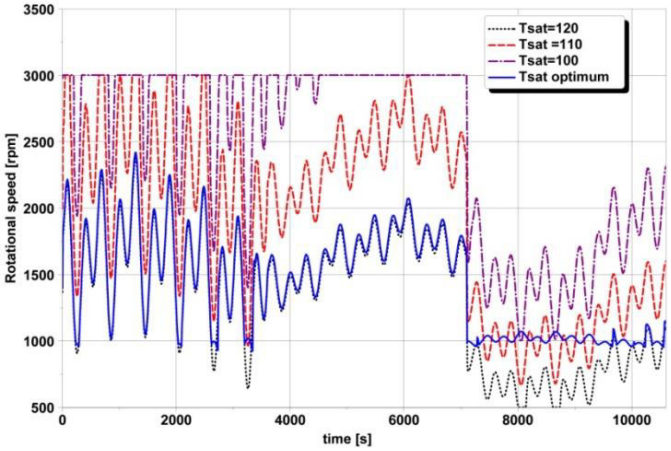

Fig. 11. Rotational speed of the expander for various saturation temperatures.

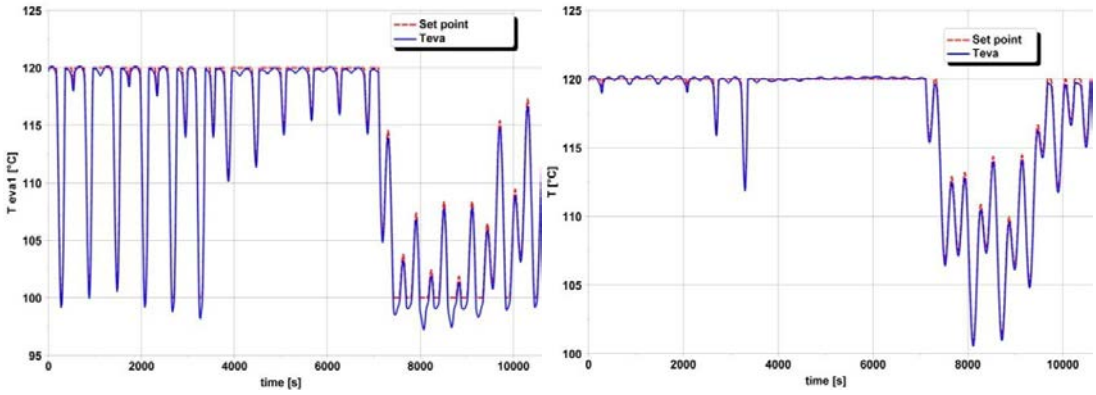

Fig. 12. Saturation temperature and set point for load cycle 1 (left) and 2 (right), strategy 3.

5.3.Start-up operations

The model was also employed to simulate a start-up operation. The available thermal power was varied from 0 to a constant value, corresponding to a flue gas stream with a mass flow rate of 0.9 kg/s and a temperature of 270°C, in 20 seconds to operate almost at the maximum power of the plant (fig. 13).

At the saturation temperature of 120°C, the production start time slightly increased respect to the other cases but, when the equilibrium was reached, the highest power output was obtained. At lower saturation temperatures the expander speed quickly reached the maximum velocity of 3000 rpm, absorbing a higher thermal power and causing a slower increase of saturation temperature, which led to a lower value of power output. The third control strategy provided a behaviour similar to the first case, with the same equilibrium power output, but the start-up process was faster than in the other cases. This analysis showed that the third control strategy is suitable for those plants where start and stop operations are frequent.

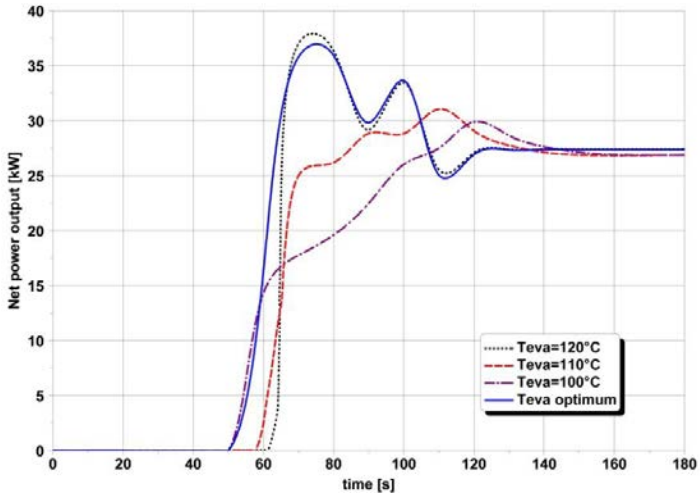

Fig. 13. Production start-up for different saturation temperatures.

6. Conclusions

An ORC cycle with a rotary expander for waste heat recovery was analysed. Firstly some stationary simulations were carried out, to select the most appropriate fluid. R-600a was the fluid which provided the highest output power in this range of temperature and applied to this type of rotary expansion device. The dynamic behaviour of the system was also simulated by imposing a variable hot flue gas temperature and mass flow rate as thermal input. The employment of superheated cycles was evaluated and results showed that this configuration led to lower efficiency of the recovery system.

Then, three different control strategies were evaluated. In the first strategy the rotational speed of the expander was kept constant. This strategy provided the worse results in terms of overall efficiency. In the second strategy the saturation temperature was kept constant by the variation of the rotational speed of the machine. This strategy gives better results, but it also requires that an optimal value of the set point is to be defined a priori as a function of the thermal input load, otherwise the overall efficiency decreased. In the third strategy, the set point of the evaporating temperature was varied through an appropriate function of the product of the volumetric flow rate to the admission pressure, to provide the maximum power output of the expander. In terms of results, this strategy was similar to the constant set point strategy, but it was also able to provide the best value of overall efficiency for different thermal input load, without the need for an a priori choice of the optimal saturation temperature.

The second and the third strategy were then used to evaluate the startup process of the system. Also in this case the second and the third strategy gave similar results in terms of delivered power, but the third strategy also provided a faster start up process. In conclusion the third strategy not only provided a slight gain in delivered power, but also had the capability of self-accommodating the optimal saturation temperature set point as well as a faster response to load variations and start and stop operations.

References

[1] Quoilin S, Declaye S, Legros A, Guillaume L, Lemort V. Working fluid selection and operating maps for Organic Rankine Cycles expansion machines. International Compressor Engineering Conference at Purdue 2012.

[2] Antonelli M, Baccioli A, Francesconi M, Desideri U, Martorano L. Operating maps of a rotary engine used as an expander for micro-generation with various working fluids. Applied Energy 2014; 113: 742-750.

[3] Rayegan R, Tao YX. A procedure to select working fluids for Solar Organic Rankine Cycles (ORCs). Renewable Energy 2010; 36: 659-670.

[4] Quoilin S, Aumann R, Grill A, Schuster A, Lemort V, Spliethoff V.. Dynamic modelling and optimal control strategy of waste heat recovery Organic Rankine Cycles. Applied Energy 2011; 88: 2183-2190.

[5] Badami M, Mura M. Preliminary design and control strategies of a small scale wood waste Rankine cycle (RC) with a reciprocating steam engine (SE). Energy 2009; 34: 1315-1324.

[6] Antonelli M, Baccioli A, Francesconi M, Martorano L. Experimental and numerical analysis of the valve timing effects on the performances of a small volumetric rotary expansion device. Energy Procedia 2014; 45: 1077-1086.

[7] Antonelli M, Martorano L. A study on the rotary steam engine for distributed generation in small size power plants. Appplied Energy 2012; 97: 642-647.

[8] Antonelli M, Baccioli A, Francesconi M, Lensi R, Martorano L. Analysis of a low concentration solar plant with compound parabolic collectors and a rotary expander for electricity generation. Energy Procedia 2014; 45: 170.179.

[9] Antonelli M, Lensi R, Martorano L. Development and validation of a numerical model of a rotary steam engine for electric power micro generation using biomass. Proceeding of the ECOS, Padova Congress 2007; 1-8.

[10] Delgado-Torres AM, Garcia-Rodriguez L. Preliminary assessment of solar organic Rankine cycles for driving a desalination system. Desalination 2007; 216: 252-275.

[11] Lakew AA, Bolland O. Working fluids for low-temperature heat source. Applied Thermal Engineering 2010; 30: 1262-1268.